Title

Dynamics of zonal shear collapse with hydrodynamic electrons

Journal

Physics of Plasmas, 25(6)

ISSN

1070-664X

Authors

Hajjar, RJ
Diamond, PH
Malkov, MA

Publication Date

2018-06-01

DOI

10.1063/1.5030345

Dynamics of zonal shear collapse with hydrodynamic electrons

R. J. Hajjar, P. H. Diamond, and M. A. Malkov

Citation: Physics of Plasmas **25**, 062306 (2018); doi: 10.1063/1.5030345
View online: https://doi.org/10.1063/1.5030345
View Table of Contents: http://aip.scitation.org/toc/php/25/6
Published by the American Institute of Physics

Dynamics of zonal shear collapse with hydrodynamic electrons

R. J. Hajjar,[1,2] P. H. Diamond,[3,4,5] and M. A. Malkov[3,4]
[1]*Department of Mechanical and Aerospace Engineering, University of California San Diego, La Jolla, California 92093, USA*
[2]*Center for Energy Research, University of California San Diego, La Jolla, California 92093, USA*
[3]*Center for Astrophysics and Space Sciences, University of California San Diego, La Jolla, California 92093, USA*
[4]*Department of Physics, University of California, San Diego, California 92093, USA*
[5]*Center for Fusion Sciences, Southwestern Institute of Physics, Chengdu, Sichuan 610041, People's Republic of China*

(Received 20 March 2018; accepted 23 May 2018; published online 8 June 2018)

This paper presents a theory for the collapse of the edge zonal shear layer, as observed at the density limit at low β. This paper investigates the scaling of the transport and mean profiles with the adiabaticity parameter α, with special emphasizes on fluxes relevant to zonal flow (ZF) generation. We show that the adiabaticity parameter characterizes the strength of production of zonal flows and so determines the state of turbulence. A 1D reduced model that self-consistently describes the spatiotemporal evolution of the mean density $\bar{n}$, the azimuthal flow $\bar{v}_y$, and the turbulent potential enstrophy $\varepsilon = \langle(\tilde{n} - \nabla^2\tilde{\phi})^2/2\rangle$—related to fluctuation intensity—is presented. Quasi-linear analysis determines how the particle flux Γ_n and vorticity flux $\Pi = -\chi_y\nabla^2 v_y + \Pi^{res}$ scale with α, in both hydrodynamic and adiabatic regimes. As the plasma response passes from adiabatic ($\alpha > 1$) to hydrodynamic ($\alpha < 1$), the particle flux Γ_n is enhanced and the turbulent viscosity χ_y increases. However, the residual flux Π^{res}—which drives the flow—drops with α. As a result, the mean vorticity gradient $\nabla^2\bar{v}_y = \Pi^{res}/\chi_y$—representative of the strength of the shear—also drops. The shear layer then collapses and turbulence is enhanced. The collapse is due to a decrease in ZF production, not an increase in damping. A physical picture for the onset of collapse is presented. The findings of this paper are used to motivate an explanation of the phenomenology of low β density limit evolution. A change from adiabatic ($\alpha = k_z^2 v_{th}^2/(|\omega|\nu_{ei}) > 1$) to hydrodynamic ($\alpha < 1$) electron dynamics is associated with the density limit. *Published by AIP Publishing.*
https://doi.org/10.1063/1.5030345

I. INTRODUCTION

Drift wave (DW) turbulence is one of the fundamental issues in magnetically confined plasmas and continues to be a subject of interest for many experimental, theoretical, and numerical studies.[1,2] Driven by radial density gradients, drift wave turbulence enhances particle and thermal transport and increases the loss of particles and heat from fusion devices. One mechanism that regulates DW fluctuations is the self-generation of sheared zonal flows (ZFs) by turbulent Reynolds stresses. These flows decorrelate turbulent eddies by shearing, thus allowing for energy transfer between disparate scales of the plasma.[3,4] ZFs are therefore often linked to *L–H* transition and internal transport barrier (ITB) formation.[5] Many models describing the regulations of DWs by ZFs have been proposed, so much so that the problem is now referred to as DW/ZF turbulence.

In another vein, there is evidence to suggest that ZFs collapse when the plasma density approaches the Greenwald density limit n_G in the *L*-mode.[6,7] This limit is an operational bound on the plasma density and represents the maximum attainable density before the plasma develops strong MHD activity.[8] Increasing the density to and above n_G leads ultimately to degradation of particle confinement and sometimes—but not always—disruption. A symptomatic series of phenomena are frequently manifested at the density limit. These include, but are not limited to: edge cooling, multifaceted asymmetric radiation from edge (MARFE), current shrinkage, and weakening of the edge shear $E \times B$ layers. Studies of the long range correlation (LRC)[6] of edge turbulence revealed a drop in LRC as $n \to n_G$, suggesting a weakening of turbulence driven zonal flows as the density limit is approached. A recent experiment in the HL-2A tokamak[7] showed that as $\bar{n}$ approaches n_G, the edge shear flow collapses. This is accompanied by an enhancement of the turbulent particle flux near the separatrix as the plasma density increases in these ohmic *L*-mode discharges. Cooling of the edge plasma and a decrease in the Reynolds force responsible for driving the zonal flow were also observed as $\bar{n}/n_G$ increased. Notably, there was a significant decrease in the adiabaticity parameter $\alpha = k_z^2 v_{th}^2/(\nu_{ei}|\omega|)$ from 3 to 0.5, as $\bar{n}$ was increased. Here, $|\omega|$ represents the frequency of the DW unstable mode. In a relevant and related vein (though not directly concerned with density limits), Schmid *et al.* deduced the weakening of zonal flow production at high collisionality. In that study, a direct experimental verification of the importance of collisionality for mesoscale (i.e., ZF) structure formation was reported, and a decrease in both

nonlinear energy transfer and the zonal flow contribution to the spectrum was observed.

A conventional approach is to attribute these observations to an increase in the plasma collisionality with $\bar{n}$ and to an increase in the damping of the ZFs.[8,9] Increasing the plasma density boosts the collisional damping of zonal flows, thus inhibiting the self-regulation of turbulence.[10–12] As a result, transport of particles and heat is enhanced and plasma confinement degrades. Alternatively, another approach links these observations to the development of additional linear instabilities, such as resistive ballooning modes, in the edge of the tokamak.[13–15] The onset of resistive ballooning modes is linked to $k_z^2 v_{th}^2/(\nu_{ei}|\omega|)$ dropping below unity. These additional instabilities are thought to enhance transport and lead to further deterioration of the plasma confinement. To this end, we note however the low values in β achieved in the HL-2A experiment mentioned above, where $0.01 < \beta < 0.02$.

Motivated by the experimental observations, we present a model that investigates turbulence and the collapse of the plasma edge shear layer in the hydrodynamic electron limit. Specifically, we present a theory for the evolution of turbulence and mean profiles (including flows) as the adiabaticity parameter α decreases below unity that is, as the plasma response passes from the adiabatic limit ($\alpha \gg 1$) to the hydrodynamic limit ($\alpha \ll 1$). Interestingly enough, findings of this paper are easily applicable to the density limit experiments, since $\alpha = k_z^2 v_{th}^2/(|\omega|\nu_{ei}) \sim T_e^{5/2}/\bar{n}$ (for $|\omega|$ fixed). For $|\omega| \sim |\omega^\star|$, as for drift wave turbulence, $\alpha \sim T_e^2/\bar{n}$ (for $k_\theta \rho_s$ fixed). For the parameters of the HL-2A experiments, it is quite unlikely that resistive ballooning modes are excited. Thus, we work within the framework of a drift wave model. A particularly simple model proposed by Hasegawa and Wakatani describes the dynamics of two-dimensional (2D) edge drift wave turbulence in a collisional plasma in the presence of a constant magnetic field. This generic system of equations describes the excitation and damping of unstable modes in terms of a few parameters related to plasma collisionality, leading to a stationary turbulence level without an external drive. In particular, the Hasegawa-Wakatani (HW) system of equations remains a valid model for edge turbulence dynamics at modest β. Although multiple studies investigating the characteristics of turbulence in the hydrodynamic limit have been published, no theoretical or physical explanation of why the shear flow collapses and/or why drift wave turbulence is enhanced for $\alpha < 1$ was presented. Recently, Schmid *et al.*[16] did present an experimental study of this subject. In fact, most studies of ZF behavior in the hydrodynamic electron regime simply appeal to numerical results that show strong turbulence and weak zonal flows in the hydrodynamic limit,[17–20] and verify the usual power laws of turbulence energy in 2D for this limit.[21]

This paper addresses these questions by presenting a simple reduced description for transport enhancement and weakening of the edge shear layer in the hydrodynamic electron limit. The model is derived from the Hasegawa-Wakatani (HW) equations for collisional drift waves, and self-consistently studies space and time evolution of the mean density $\bar{n}$, mean azimuthal flow $\bar{v}_y$, and turbulent potential enstrophy ε. The model determines the role of the Reynolds stress $\langle \tilde{v}_x \tilde{v}_y \rangle$ in the feedback loop between flows and turbulence and gives additional insight into the DW/ZF relation in the hydrodynamic electron limit. Quasi-linear analysis shows that both the particle flux Γ_n and the turbulent viscosity χ_y are enhanced as α decreases. However, the residual vorticity stress Π^{res}, which accelerates the flow, is reduced as α increases. The mean vorticity gradient equal to Π^{res}/χ_y is then reduced, and the edge shear layer collapses. As a result, transport of particles and heat increases. These findings are relevant to the density limit experiment, as $\alpha \propto T_e^2/\bar{n}$. When $\bar{n}$ increases, α decreases, and Π^{res}/χ_y is reduced. The plasma production of zonal flows declines and turbulence and transport increase. Thermal and particle transport increases, thereby triggering cooling of the edge plasma, in part because of inward turbulence spreading. For constant pressure, a drop in plasma temperature T_e leads to a further increase in the density and feedback loop between T_e and $\bar{n}$ forms.

We give a physical explanation of zonal flow collapse based on energy and momentum density flux behavior in the adiabatic and hydrodynamic regimes. In the adiabatic regime, the momentum flux scales as $\langle \tilde{v}_x \tilde{v}_y \rangle \propto -\langle k_r k_\theta \rangle$, where k_r and k_θ are the radial and azimuthal wavenumbers, respectively. The group velocity v_{gr}, at which the wave energy density propagates $\langle v_{gr} \varepsilon \rangle$, scales as $v_{gr} \propto -\langle k_r k_\theta \rangle v_d$, where the electron diamagnetic velocity $v_d < 0$. With $v_{gr} > 0$, the relation between the flux of wave energy density and momentum implies a counter-flow spin up, i.e., an incoming wave momentum flux occurs for an outgoing wave energy density flux as shown in Fig. 1. Alternatively put, a system of drift wave—zonal flow turbulence naturally tends to converge zonal momentum into regions of wave excitation, from which wave energy radiates. This promotes the production of zonal flows in the adiabatic regime. In the

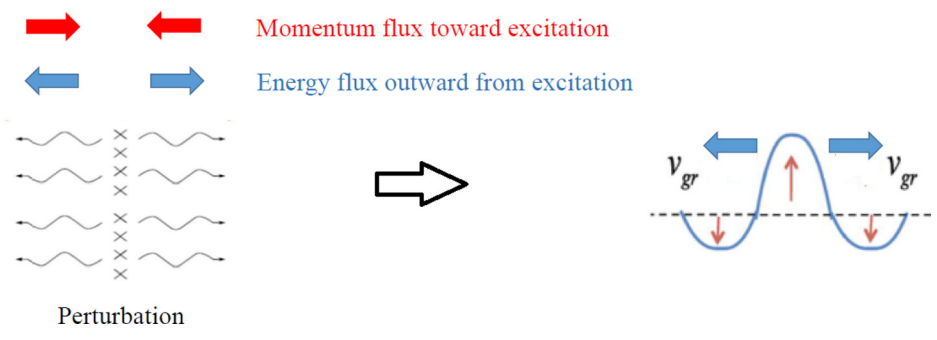

FIG. 1. Outgoing wave energy flux and incoming momentum flux from/to perturbation in the adiabatic regime.

hydrodynamic limit however, the group velocity does not scale directly with k_θ. Thus, the strong link between the two fluxes is broken, and so the familiar pattern of zonal flow amplification in regions from which wave energy radiates no longer holds. The familiar tilt-and-stretch mechanism does not apply. This simple idea explains why zonal flows are not produced in the hydrodynamic regime. We comment here that the topic of density limits is an extremely complex and broad one, involving many different physical processes.[9] The scenario analyzed here is relevant but not universal. Other explanations are possible. In particular, the physics of *H*-mode density limits, which are necessarily coupled to the $H \to L$ back transition, requires significant further consideration.

The rest of this paper is organized as follows: Sec. II gives the linear response analysis of the basic Hasegawa-Wakatani system, as well as solution of the DW dispersion relation in both the adiabatic and hydrodynamic limits. Section III introduces the reduced model used to describe the evolution of the three fields: $\bar{n}$, $\bar{v}_y$, and ε. In Sec. IV, we calculate the expressions for the particle flux, the vorticity flux, and the Reynolds work in both adiabatic and hydrodynamic limits. The latter reflects the potential enstrophy exchange between fluctuations and mean flow. The model is then simplified to a predator/prey model by slaving the expression for ε in the equations for $\bar{n}$ and $\bar{v}_y$ in Sec. V. Section VI gives a physical argument as to why zonal flow formation is weak in the hydrodynamic limit. Variations of the mean vorticity gradient Π^{res}/χ_y, as well as changes in the scaling of the vorticity flux $\langle \tilde{v}_x \nabla_\perp^2 \phi \rangle$, are examined, in order to characterize the mesoscopic plasma response as α decreases. The drop in zonal flow drive is reconciled with the persistence of potential vorticity (PV) mixing in the hydrodynamic limit. Section VII interprets the experimental observations obtained in density limit experiments and in studies of edge turbulence at high collisionality from the perspective of the collapse of ZFs in the hydrodynamic electron limit. A scenario linking shear layer collapse to the density limit is suggested. Finally, conclusions and future work are discussed in Sec. VIII.

II. BASIC SYSTEM AND LINEAR STABILITY ANALYSIS

In a box of dimensions: $0 \le x \le L_x$, $0 \le y \le L_y$, $0 \le z \le L_z$, the equations for the density n and vorticity $\nabla^2\phi$ in a nonuniform plasma with density $n_0(x)$ and constant magnetic field $\mathbf{B} = B\hat{z}$ are[22]

$$\frac{dn}{dt} = -\frac{v_{th}^2}{\nu_{ei}} \nabla_\parallel^2 (\phi - n) + D_0 \nabla^2 n, \tag{1a}$$

$$\frac{d\nabla^2\phi}{dt} = -\frac{v_{th}^2}{\nu_{ei}} \nabla_\parallel^2 (\phi - n) + \mu_0 \nabla^2 (\nabla^2 \phi). \tag{1b}$$

Here, the fields are normalized as: $n \equiv n/n_0$, $\phi \equiv e\phi/T_e$, $t \equiv \omega_{ci} t$, $length \equiv length/\rho_s$, $v_{th} \equiv v_{th}/c_s$, and $\nu_{ei} \equiv \nu_{ei}/\omega_{ci}$. The average plasma density, the electron temperature, and thermal velocity, as well as the plasma sound speed, are n_0, T_e, v_{th}, and c_s, respectively. ω_{ci} is the ion cyclotron frequency, and $\rho_s = c_s/\omega_{ci}$ is the ion Larmor radius with temperature T_e. The collisional diffusion coefficients D_0 and μ_0 dissipate energy at small scales by frictional drag through forward energy cascade. The electron parallel diffusion rate $\hat{\alpha} = -v_{th}^2 \nabla_\parallel^2/\nu_{ei} = k_z^2 v_{th}^2/\nu_{ei}$ couples the vorticity fluctuations to those in the density profile. The convective derivative is equal to: $d/dt = \partial_t + (\hat{z} \times \nabla\phi).\nabla = \partial_t + v_E.\nabla$ where v_E is the $E \times B$ drift. The fields are decomposed into a perturbation and a zonally averaged part: $f = \bar{f}(x,t) + \tilde{f}(x,y,z,t)$, where the averaging is preformed over the directions of symmetry y and z

$$\langle f \rangle = \bar{f} = \frac{1}{L_y L_z} \int_0^{L_y} \int_0^{L_z} f dy dz.$$

Equations for the density and vorticity fluctuations are written as

$$\partial_t \tilde{n} + \tilde{v}_x.\nabla\bar{n} = -\frac{v_{th}^2}{\nu_{ei}} \nabla_\parallel^2 (\tilde{\phi} - \tilde{n}) - \{\tilde{\phi}, \tilde{n}\} + D_0 \nabla^2 \tilde{n}, \tag{2a}$$

$$\partial_t \nabla^2 \tilde{\phi} + \tilde{v}_x.\nabla\overline{\nabla^2\phi} = -\frac{v_{th}^2}{\nu_{ei}} \nabla_\parallel^2 (\tilde{\phi} - \tilde{n}) - \{\tilde{\phi}, \nabla^2\tilde{\phi}\} + \mu_0 \nabla^2 (\nabla^2 \tilde{\phi}). \tag{2b}$$

Here, the mean flow shear $\overline{\nabla^2\phi}$ in Eq. (2b) is self-generated by the Reynolds stress $\langle \tilde{v}_x \tilde{v}_y \rangle$ and is driven by the DW interactions. Based on the triad coupling, this internal shear results from nonlinear energy transfer related, but not identical to, the inverse energy cascade in a 2D fluid. The nonlinear advection terms are expressed as Poisson brackets: $\{f, g\} = \partial_x f \partial_y g - \partial_y f \partial_x g$ and represent spatial scattering of the fluctuation energy.

In the Hasegawa-Wakatani (HW) system, the plasma response and the character of the flow are mainly determined by three parameters: the collisional diffusion coefficients D_0 and μ_0, and the adiabaticity parameter $\alpha = k_z^2 v_{th}^2/(\nu_{ei}|\omega|)$. While D_0 and μ_0 regulate the dissipation of energy at small scales, α determines the efficiency of zonal flow production and controls its mesoscopic response. Defined as the ratio between the parallel diffusion rate and the drift frequency, α controls the phase difference between $\tilde{\phi}$ and $\tilde{n}$, and thus the transport. When $\alpha > 1$, the plasma response is near adiabatic, $\tilde{\phi}$ and $\tilde{n}$ are closely coupled, and $\tilde{n} \simeq \tilde{\phi}$. The Hasegawa-Wakatani system effectively reduces then to the Hasegawa-Mima equation[23] with a phase shift between $\tilde{n}$ and $\tilde{\phi}$. In the opposite limit however, $\alpha < 1$, the plasma response is said to be hydrodynamic. Equations (2a) and (2b) are then weakly coupled, and the $\tilde{n}$ dynamics resembles that of a passive scalar. Moreover, the vorticity equation tends toward that for a 2D Navier-Stokes fluid.[19]

For a linear stability analysis of the HW equations, we write the fluctuation fields as: $\tilde{f}_m = \delta f_m(x) e^{i[k_\theta y + k_z z - \omega t]}$ with $\omega = \omega^r + i|\gamma_m|$. Here ω^r, $|\gamma_m|$, k_θ, and k_z are the linear eigenfrequency, the growth rate, the azimuthal, and the parallel wavenumbers of the unstable mode, respectively. The drift wave dispersion relation is then

$$\omega^2 + i\frac{\hat{\alpha}}{k_\perp^2 \rho_s^2} \left[\omega(1 + k_\perp^2 \rho_s^2) - \omega^\star\right] = 0, \tag{3}$$

where $\omega^\star = k_\theta |v_d| = -k_\theta \rho_s c_s \nabla\bar{n} > 0$ is the electron drift frequency, and $v_d = \rho_s c_s \nabla\bar{n} < 0$ is the electron diamagnetic drift velocity. The solution of Eq. (3) is given by

$$\omega = \frac{1}{2}\left(-i\frac{\hat{\alpha}(1+k_\perp^2\rho_s^2)}{k_\perp^2\rho_s^2} + \sqrt{\frac{4i\omega^\star\hat{\alpha}}{k_\perp^2\rho_s^2} - \left(\frac{\hat{\alpha}(1+k_\perp^2\rho_s^2)}{k_\perp^2\rho_s^2}\right)^2}\right). \tag{4}$$

This expression is simplified, according to the magnitude of $\hat{\alpha}/|\omega|$, i.e., the magnitude of α. *In the adiabatic limit:* ($\alpha \gg 1$ and $\hat{\alpha} \gg |\omega|$).

When the parallel diffusion rate $k_z^2 v_{th}^2/\nu_{ei}$ is larger than both the drift frequency $|\omega|$ and the electron diamagnetic frequency $|\omega^\star|$, Eq. (4) reduces to

$$\omega_{adiabatic} = \frac{\omega^\star}{1+k_\perp^2\rho_s^2} + i\frac{\omega^{\star 2}k_\perp^2\rho_s^2}{\hat{\alpha}}. \tag{5}$$

In the adiabatic limit, ω^r does not depend on $\hat{\alpha}$. However, the growth rate $|\gamma_m|$ is proportional to $1/\hat{\alpha}$. For large $\hat{\alpha}$, the growth rate is $|\gamma_m| \ll 1$, and the drift wave eigenfrequency is simply written as

$$\omega_{adiabatic} \simeq \omega^r = \omega^\star(1+k_\perp^2\rho_s^2)^{-1}. \tag{6}$$

In the hydrodynamic limit: ($\alpha \ll 1$ and $\hat{\alpha} \ll |\omega|$).

When the parallel diffusion rate $k_z^2 v_{th}^2/\nu_{ei}$ is much smaller than $|\omega|$, the expression for the frequency reads

$$\omega_{hydrodynamic} \simeq \frac{1}{2}\left(-i\frac{\hat{\alpha}(1+k_\perp^2\rho_s^2)}{k_\perp^2\rho_s^2} + \sqrt{\frac{4i\hat{\alpha}\omega^\star}{k_\perp^2\rho_s^2}}\right)$$
$$\simeq \sqrt{\frac{\omega^\star\hat{\alpha}}{2k_\perp^2\rho_s^2}}(1+i). \tag{7}$$

In this limit, the growth rate and the real part are both equal to: $\omega^r = |\gamma_m| = \sqrt{\omega^\star\hat{\alpha}/2k_\perp^2\rho_s^2}$. In contrast to the adiabatic limit, the contribution of $|\gamma_m|$ cannot be neglected in the expression for $\omega_{hydrodynamic}$.

A comparison of Eqs. (6) and (7) shows that $\omega_{adiabatic}$ is dominantly real, while $\omega_{hydrodynamic}$ involves a comparable real and imaginary part. While the motion of the drift waves is purely oscillatory in the adiabatic limit, in the hydrodynamic limit, the dynamics of the perturbation resembles that of a convective cell. This feature dictates the behavior of the flow in the two plasma regimes.

III. REDUCED MODEL

A. The equations

In this section, a 1D reduced model that self-consistently describes the evolution of turbulence and plasma profiles is presented. The equations relating the time and space evolution of the plasma mean density $\bar{n}$ and mean vorticity $\overline{\nabla^2\phi}$ are obtained by averaging Eqs. (1a) and (1b) over the directions of symmetry

$$\partial_t\bar{n} = -\partial_x\langle\tilde{v}_x\tilde{n}\rangle + D_0\nabla^2\bar{n}, \tag{8a}$$

$$\partial_t\overline{\nabla^2\phi} = -\partial_x\langle\tilde{v}_x\nabla^2\tilde{\phi}\rangle - \nu_{in}(\bar{v}_y - \bar{v}_n) + \mu_0\nabla^2\overline{\nabla^2\phi}. \tag{8b}$$

A neutral damping term proportional to the ion-neutral collision frequency $\nu_{in} \propto n_n$ is added to the mean vorticity equation. This term can be significant at the plasma edge. It is a sink of energy transferred to larger scales and so damps the zonal flows. The neutral friction can be dropped from the mean vorticity equation if $\nu_{in} \to 0$, i.e., for low neutral density n_n.

In addition to Eqs. (8a) and (8b), we formulate an equation for the fluctuation potential enstrophy $\varepsilon = \langle(\tilde{n} - \nabla^2\tilde{\phi})^2/2\rangle$. The HW system locally conserves the potential vorticity defined as $q = n - \nabla^2\phi$, up to viscosity and particle diffusivity. A linearized equation describing the time evolution of the turbulent potential vorticity $\tilde{q} = \tilde{n} - \nabla^2\tilde{\phi}$ is obtained by subtracting Eq. (2b) from Eq. (2a)

$$\frac{\partial\tilde{q}}{\partial t} + \tilde{v}_x.\nabla\bar{q} = -\{\tilde{\phi},\tilde{q}\} + \mu_0\nabla^2 q \Rightarrow \frac{dq}{dt} = \mu_0\nabla^2 q, \tag{9}$$

where $q = \bar{q} + \tilde{q}$, and μ_0 and D_0 are assumed to be of the same order. Equation (9) represents the conservation of the total potential vorticity up to viscous dissipation. Therefore, the potential enstrophy $\varepsilon = \langle\tilde{q}^2\rangle/2 = \langle(\tilde{n} - \nabla^2\tilde{\phi})^2\rangle/2$ is also conserved up to collisional diffusion. This can be shown by multiplying Eq. (9) by $\tilde{q} = \tilde{n} - \nabla^2\tilde{\phi}$, and performing a zonal integral. Detailed calculations can be found in Refs. 24–26. Here, we simply write the time evolution equation for the potential enstrophy density ε

$$\partial_t\varepsilon + \partial_x\Gamma_\varepsilon = -(\Gamma_n - \Pi)(\partial_x\bar{n} - \partial_{xx}\bar{v}_y) - \varepsilon^{3/2} + P. \tag{10}$$

In Eq. (10), Γ_n and Π are the particle and vorticity flux, respectively, while $\partial_x\bar{n}$ and $\partial_{xx}\bar{v}_y$ are the mean density and mean vorticity gradients, respectively. The turbulent potential enstrophy density flux Γ_ε on the LHS represents the mesoscopic spreading of turbulence due to the three wave coupling. Note that $\Gamma_\varepsilon = \langle\tilde{v}_x\varepsilon\rangle$ is nominally third order in fluctuation amplitude. It thus is equivalent to the spatial flux of turbulence intensity—otherwise known as "turbulence spreading." The spreading flux Γ_ε represents local scattering of the fluctuation potential enstrophy density ε. Turbulence spreading enters here as a consequence of: (i) the fact that the model conserves potential vorticity and thus potential enstrophy, (ii) the fact that local potential enstrophy density evolution is determined (in part) by the divergence of the flux of local potential enstrophy. The potential enstrophy density flux is written as: $\Gamma_\varepsilon = -D_\varepsilon\partial_x\varepsilon = -l_{mix}^2\sqrt{\varepsilon}\partial_x\varepsilon$, where $l_{mix} = \tilde{v}_x\tau_c$ is the turbulent mixing length and τ_c is the turbulence correlation time. The first term on the RHS of Eq. (10) accounts for direct mean flow-fluctuation coupling and converts the mean potential enstrophy into fluctuation potential enstrophy. This coupling term relates variations of the turbulent potential enstrophy to those in the mean profile of $\bar{n}$ and $\bar{v}_y$, via the particle flux $\Gamma_n = \langle\tilde{v}_x\tilde{n}\rangle$ and the vorticity flux $\Pi = \langle\tilde{v}_x\nabla^2\tilde{\phi}\rangle$. The second term on the RHS of Eq. (10) represents the dissipation of fluctuation potential enstrophy density at a rate $\sqrt{\varepsilon}$. This dissipation is due ultimately to the collisional coefficients D_0 and μ_0. Finally, the production term P represents an input of the potential enstrophy due to linear growth, driven by the mean profiles. It is proportional to ε and linear in γ_{DW}, the growth rate of the DW instability: $P = \gamma_{DW}\varepsilon$. Dropping the neutral damping term from the

vorticity equation, as well as the $\bar{..}$ sign, we simplify the notation by writing $u = \overline{\nabla^2\phi}$ to obtain

$$\partial_t n = -\partial_x \Gamma_n + D_0 \nabla^2 n, \tag{11a}$$

$$\partial_t u = -\partial_x \Pi + \mu_0 \nabla^2 u, \tag{11b}$$

$$\partial_t \varepsilon + \partial_x \Gamma_\varepsilon = -(\Gamma_n - \Pi)(\partial_x n - \partial_x u) - \varepsilon^{3/2} + P. \tag{11c}$$

Written in 1D (in radius), this system models the evolution of DW intensity and the formation of zonal flows in the plasma. For this purpose, an expression for the mixing length l_{mix} is required.

One approach consists of considering a mixing length that exhibits a turbulence suppression through the azimuthal shear $u = \nabla v_y$

$$l_{mix} = \frac{l_0}{\left(1 + \frac{(l_0 \nabla u)^2}{\varepsilon}\right)^\delta}, \tag{12}$$

where δ is a free parameter and l_0 is an external dynamical turbulence production scale length. Equation (12) exhibits a decorrelation of the turbulent structures by the flow shear $u = \nabla v_y$:[27] when the flow shear increases, the mixing length decreases. When l_{mix} is reduced, the production of potential enstrophy ε also drops, the mean profiles steepen, and a closed feedback loop is obtained. In the particular case of weak or collapsed flow shear, $u = \nabla v_y$ is small ($u = \nabla v_y \simeq 0$) so a constant mixing length $l_{mix} \simeq l_0$ is appropriate. This is a consequence of the absence of transport barrier dynamics in the phenomena of interest.

IV. EXPRESSIONS FOR THE TURBULENT FLUXES

In addition to the expression for l_{mix}, expressions for the turbulent fluxes $\langle \tilde{v}_x \tilde{n} \rangle$ and $\langle \tilde{v}_x \tilde{v}_y \rangle$ are needed to close the model and solve Eqs. (11a)–(11c). In this section, we use quasi linear theory to calculate the expressions for the particle flux and vorticity flux.

A. The particle flux: $\langle \tilde{n}\tilde{v}_x \rangle$

To calculate the expression for the particle flux $\langle \tilde{n}\tilde{v}_x \rangle$, we write the electron density fluctuation as $\tilde{n} = \tilde{\phi} + h$, where h is the deviation from the adiabatic response. Plugging in Eq. (2a), we obtain

$$h = \frac{\omega^\star - \omega}{\omega + i\hat{\alpha}} \tilde{\phi}, \quad \tilde{n} = \tilde{\phi} + h = \left(\frac{\omega^\star + i\hat{\alpha}}{\omega + i\hat{\alpha}}\right)\tilde{\phi}.$$

In the adiabatic limit, $\omega \simeq \omega^\star$ and the following relation between $\tilde{n}$ and $\tilde{\phi}$ is recovered: $\tilde{n} = (1 - i(\omega^\star - \omega)/\hat{\alpha})\tilde{\phi} \simeq \tilde{\phi}$.[28] For $\tilde{v}_x = -ik_\theta \rho_s c_s \delta\phi$, the expression for the particle flux $\langle \tilde{n}\tilde{v}_x \rangle$ is

$$\begin{aligned}\Gamma_n &= -\left[\frac{(\hat{\alpha} + |\gamma_m|)}{|\omega + i\hat{\alpha}|^2}\frac{d\ln n}{dx} + \frac{\hat{\alpha}\omega^r}{k_\theta \rho_s c_s |\omega + i\hat{\alpha}|^2}\right]\langle \delta v_x^2 \rangle \\ &\simeq -\frac{(\hat{\alpha} + |\gamma_m|)}{|\omega + i\hat{\alpha}|^2}\frac{d\ln n}{dx}\langle \delta v_x^2 \rangle = -\frac{D}{n_0}\frac{d\bar{n}}{dx}.\end{aligned} \tag{13}$$

The particle diffusion coefficient is: $D = [(\hat{\alpha} + |\gamma_m|)/|\omega + i\hat{\alpha}|^2]\langle \delta v_x^2 \rangle$. The expression for the particle diffusion coefficient D depends on $\hat{\alpha}$ and changes as the plasma passes from the adiabatic to the hydrodynamic regime. We introduce next the factor f that represents the fraction of the fluctuation energy εl_{mix}^2 which is in the kinetic energy of radial motion

$$\langle \delta v_x^2 \rangle = f \varepsilon l_{mix}^2 = \frac{\langle \delta v_x^2 \rangle}{\langle \delta n^2 \rangle + \langle \delta v_x^2 \rangle}\varepsilon l_{mix}^2. \tag{14}$$

Using the expressions for $\tilde{n}$ and $\tilde{v}_x$, the expression for f is equal to

$$\begin{aligned} f &= \frac{k_\perp^2 \rho_s^2}{\left|\frac{\omega^* + i\hat{\alpha}}{\omega + i\hat{\alpha}}\right|^2 + k_\perp^2 \rho_s^2} \\ &= \begin{cases} \dfrac{k_\perp^2 \rho_s^2}{1 + k_\perp^2 \rho_s^2}, & \text{in the adiabatic regime} \\ \dfrac{1}{|\omega^*/\hat{\alpha}| + 1}, & \text{in the hydrodynamic regime.} \end{cases} \end{aligned} \tag{15}$$

In the adiabatic regime, the kinetic energy $\langle \delta v_x^2 \rangle$ is less than $\langle \delta n^2 \rangle$, and the electron total energy is mostly thermal/internal energy. Therefore, the factor $f \ll 1$. However, in the hydrodynamic regime, the kinetic energy of the electrons rises as compared to $\langle \delta n^2 \rangle$, reflecting an increase in the screening of ion diamagnetic oscillations such that $f \to 1$. For small values of $k_\perp^2 \rho_s^2 \ll 1$, the two limits of f are

$$\begin{cases} f \to k_\perp^2 \rho_s^2, & \text{in the adiabatic regime} \\ f \to 1, & \text{in the hydrodynamic regime.} \end{cases}$$

Finally, for purely adiabatic DWs, the relation $\langle \delta v_x^2 \rangle \simeq k_\perp^2 \rho_s^2 \varepsilon l_{mix}^2$ is recovered.

B. The vorticity flux: $\langle \tilde{v}_x \nabla_\perp^2 \phi \rangle$

In addition to Γ_n, we calculate the vorticity flux $\Pi = \langle \tilde{v}_x \nabla_\perp^2 \tilde{\phi} \rangle$. This flux is related to the Reynolds force that controls the relation between turbulence and zonal flows via the Taylor identity: $-\partial_x \langle \tilde{v}_x \tilde{v}_y \rangle = \langle \tilde{v}_x \nabla_\perp^2 \tilde{\phi} \rangle$. The Taylor identity directly links the zonal flow momentum conservation to potential enstrophy balance.[29] To calculate Π, we use the vorticity equation and drop the neutral drag term for simplicity. The vorticity flux then follows as:

$$\begin{aligned} \Pi &= \sum_m -\frac{k_\theta^2 \rho_s^2 c_s^2 |\gamma_m|}{|\omega|^2} |\tilde{\phi}^2| \frac{d^2 \bar{v}_y}{dx^2} \\ &\quad + 2Re\left[\frac{k_\theta \rho_s c_s \hat{\alpha}}{\omega}\left(\frac{\omega^\star - \omega}{\omega + i\hat{\alpha}}\right)|\tilde{\phi}|^2\right] \\ &= -\chi_y \frac{d\langle \nabla_\perp^2 \phi \rangle}{dx} + \Pi^{res} \\ &= -\chi_y \frac{d^2 \bar{v}_y}{dx^2} + \Pi^{res}, \end{aligned} \tag{16}$$

The first term of Eq. (16) represents the diffusive flux, while the second term is the residual stress, i.e., the non-diffusive flux driven by ∇n. The turbulent viscosity χ_y relating the

mean vorticity gradient $d(\nabla\bar{v}_y)/dx$ to the vorticity flux Π is equal to

$$\chi_y = \sum_m \frac{k_\theta^2\rho_s^2c_s^2|\gamma_m|}{|\omega|^2}|\tilde{\phi}^2| = \frac{|\gamma_m|\langle\delta v_x^2\rangle}{|\omega|^2}. \tag{17}$$

Here, χ_y depends on the adiabaticity parameter, as both $|\gamma_m|$ and $|\omega|$ are $\hat{\alpha}$-dependent. The residual stress Π^{res} resulting from coupling between the density and vorticity profiles is equal to

$$\Pi^{res} = \frac{k_\theta\rho_sc_s\omega_{ci}\hat{\alpha}[(\omega^r)^2(\omega^\star-\omega^r) - |\gamma_m|^2(\omega^r+\omega^\star) - \omega^\star\hat{\alpha}|\gamma_m|]}{|\omega|^2\times|\omega+i\hat{\alpha}|^2}\langle\tilde{\phi}^2\rangle. \tag{18}$$

Π^{res} converts the driving particle flux into zonal (azimuthal) flow and can accelerate $\bar{v}_y$ from rest. Similar to the expression for χ_y, Π^{res} varies as $\hat{\alpha}$ changes, affecting thereby the character of the flow in both plasma limits. In the adiabatic limit, an examination of the expression for Π^{res} shows that the residual stress is inversely proportional to $\hat{\alpha}$, i.e., $\Pi^{res}_{adia}\propto 1/\hat{\alpha}$. In the hydrodynamic limit however, the residual stress is directly proportional to $\sqrt{\hat{\alpha}}$, i.e., $\Pi^{res}_{hydro}\propto\sqrt{\hat{\alpha}}$, for $\alpha\ll 1$.

C. Fluxes and Reynolds work in adiabatic and hydrodynamic limits

The expressions for the particle and vorticity flux can be simplified depending on the value of $\hat{\alpha}$, i.e., depending on the electron plasma response.

In the adiabatic limit: ($\hat{\alpha}\gg|\omega|$).

In this limit, $\alpha\gg 1$. The growth rate $|\gamma_m|\simeq 1/\alpha\ll 1$, and $|\omega|^2\simeq(\omega^r)^2=[\omega^\star/(1+k_\perp^2\rho_s^2)]^2$. The expressions for the particle and vorticity fluxes in the adiabatic limit are

$$n_0\Gamma_n = -\frac{\langle\delta v_x^2\rangle}{\hat{\alpha}}\frac{d\bar{n}}{dx}\simeq -\frac{\varepsilon l_{mix}^2}{\hat{\alpha}}\frac{d\bar{n}}{dx}, \tag{19a}$$

$$\begin{aligned}\Pi &= -\frac{|\gamma_m|\langle\delta v_x^2\rangle}{|\omega|^2}\frac{d^2\bar{v}_y}{dx^2} - \frac{\omega_{ci}\langle\delta v_x^2\rangle}{\hat{\alpha}}\frac{d\bar{n}}{dx}\left(\frac{k_\perp^2\rho_s^2}{1+k_\perp^2\rho_s^2}\right)\\ &\simeq -\frac{\varepsilon l_{mix}^2}{\hat{\alpha}}\frac{d^2\bar{v}_y}{dx^2} - \frac{\omega_{ci}\varepsilon l_{mix}^2}{\hat{\alpha}}\frac{d\bar{n}}{dx}.\end{aligned} \tag{19b}$$

Here, $\langle\delta v_x^2\rangle_{adiabatic}=f_{adiabatic}\varepsilon l_{mix}^2=k_\perp^2\rho_s^2\varepsilon l_{mix}^2/(1+k_\perp^2\rho_s^2)$. Scalings of the particle flux Γ_n, the turbulent viscosity χ_y and the residual stress Π^{res} in the adiabatic limit are

$$\Gamma_n\simeq -(\varepsilon l_{mix}^2/\hat{\alpha})\nabla\bar{n}, \tag{20a}$$

$$\chi_y\simeq\varepsilon l_{mix}^2/\hat{\alpha}, \tag{20b}$$

$$\Pi^{res}\simeq -(\omega_{ci}\varepsilon l_{mix}^2/\hat{\alpha})\nabla\bar{n}. \tag{20c}$$

Here, Γ_n, χ_y, and Π^{res} are all inversely proportional to α. In addition, both Γ_n and Π^{res} are proportional to ∇n. The expression for the Reynolds power density P_{Re} that represents the power exerted by the turbulence on the flow $\bar{v}_y$ is obtained by multiplying the Reynolds force $F_{Re}=-\partial_x\langle\tilde{v}_x\tilde{v}_y\rangle$ by the azimuthal flow $\bar{v}_y$. In the adiabatic limit, P_{Re} is equal to

$$P_{Re} = -\partial_x\langle\tilde{v}_x\tilde{v}_y\rangle\bar{v}_y\simeq\left(-\frac{\varepsilon}{\hat{\alpha}}\frac{d^2\bar{v}_y}{dx^2} - \frac{\omega_{ci}\varepsilon}{\hat{\alpha}}\frac{d\bar{n}}{dx}\right)\bar{v}_y l_{mix}^2. \tag{21}$$

In the (likely case of) absence of an external azimuthal momentum source, and for vanishing Reynolds power density $P_{Re}=0$, the mean vorticity gradient is independent of $\hat{\alpha}$ and is given by

$$\frac{d^2\bar{v}_y}{dx^2} = \frac{\Pi^{res}}{\chi_y} = -\omega_{ci}\frac{d\bar{n}}{dx}. \tag{22}$$

In the hydrodynamic limit: ($\hat{\alpha}\ll|\omega|$) For $\omega^r=|\gamma_m|=\sqrt{\omega^\star\hat{\alpha}/(2k_\perp^2\rho_s^2)}$, expressions for the particle and vorticity fluxes are equal to

$$n_0\Gamma_n\simeq -\sqrt{\frac{k_\perp^2\rho_s^2}{2k_\theta\rho_sc_s}}\sqrt{\frac{|d\bar{n}/dx|}{\hat{\alpha}}}\langle\delta v_x^2\rangle\simeq -\frac{\varepsilon l_{mix}^2}{\sqrt{\hat{\alpha}|\omega^\star|}}\frac{d\bar{n}}{dx} \tag{23a}$$

$$\begin{aligned}\Pi &= -\frac{|\gamma_m|\langle\delta v_x^2\rangle}{|\omega|^2}\frac{d^2\bar{v}_y}{dx^2} - \frac{\omega_{ci}\langle\delta v_x^2\rangle}{k_\theta\rho_sc_s}\cdot\sqrt{\frac{k_\perp^2\rho_s^2}{2}}\sqrt{\frac{\hat{\alpha}}{|\omega^\star|}}\\ &\simeq -\frac{\varepsilon l_{mix}^2}{\sqrt{\hat{\alpha}|\omega^\star|}}\frac{d^2\bar{v}_y}{dx^2} - \frac{\omega_{ci}\varepsilon\sqrt{\hat{\alpha}}l_{mix}^2}{|\omega^\star|^{3/2}}\frac{d\bar{n}}{dx}.\end{aligned} \tag{23b}$$

Here, we used $\langle\delta v_x^2\rangle_{hydrodynamic}=f_{hydrodynamic}\varepsilon l_{mix}^2=\varepsilon l_{mix}^2/[|\omega^*/\hat{\alpha}|+1]<\varepsilon l_{mix}^2$. Scalings of the turbulent fluxes are then

$$\Gamma_n\simeq -\left(\varepsilon l_{mix}^2/\sqrt{\hat{\alpha}|\omega^\star|}\right)\nabla\bar{n}, \tag{24a}$$

$$\chi_y\simeq\varepsilon l_{mix}^2/\sqrt{\hat{\alpha}|\nabla\bar{n}|}, \tag{24b}$$

$$\Pi^{res}\simeq -\left(\omega_{ci}\varepsilon\sqrt{\hat{\alpha}}l_{mix}^2/|\omega^\star|^{3/2}\right)\nabla\bar{n}. \tag{24c}$$

While Γ_n and χ_y are inversely proportional to $\sqrt{\hat{\alpha}}$ in the hydrodynamic limit, the residual stress Π^{res} scales proportionally with $\sqrt{\hat{\alpha}}$. We note here that in the hydrodynamic limit, the particle flux Γ_n^{hydro} is proportional to $\sqrt{|\nabla\bar{n}|}$, and the residual stress Π^{res}_{hydro} is proportional to $1/\sqrt{|\nabla\bar{n}|}$. Such superficially unusual scalings with $|\nabla\bar{n}|$ result from neglecting the contributions of the diffusive damping related to D_0 and μ_0 in the density and vorticity equations, while performing the linear analysis. Obviously, these should not be extrapolated to regimes of very weak ∇n drive. In the hydrodynamic limit, the Reynolds power density is equal to

$$P_{Re} = -\partial_x \langle \tilde{v}_x \tilde{v}_y \rangle \bar{v}_y \simeq \left(-\frac{\varepsilon}{\sqrt{\hat{\alpha}|\nabla \bar{n}|}} \frac{d^2 \bar{v}_y}{dx^2} - \omega_{ci} \varepsilon \sqrt{\frac{\hat{\alpha}}{|\nabla \bar{n}|}} \right) \bar{v}_y l_{mix}^2, \tag{25}$$

and the vorticity gradient for $P_{Re} = 0$ is directly proportional to $\hat{\alpha}$ and is equal to

$$\frac{d^2 \bar{v}_y}{dx^2} = -\frac{\omega_{ci} \hat{\alpha}}{|\omega^\star|} \frac{d\bar{n}}{dx}. \tag{26}$$

V. SIMPLIFICATION BY SLAVING: A PREDATOR-PREY MODEL

When the eddy turnover time $\tau_c = l_{mix}/\tilde{v}_x$ is smaller than the particle confinement time $[D\nabla^2 \bar{n}/\bar{n}]^{-1}$, the model can be reduced to a 2-field predator-prey model that evolves the preys ($\bar{n}$) and predators ($\bar{v}_y$) according to Eqs. (11a) and (11b). Clearly, these predators do not exist without the prey. A simplification of the previous model is achieved by slaving the expression for ε to the mean profiles, and solving the equations for $\bar{n}$ and $\bar{v}_y$. For slaved turbulence, both potential enstrophy spreading and potential enstrophy production are dropped from the ε equation because the eddy turnover time is shorter than the confinement time. The potential enstrophy equation then reduces to the balance

$$-(\Gamma_n - \Pi)(\partial_x n - \partial_x u) - \varepsilon^{3/2} = 0. \tag{27}$$

In the adiabatic limit: using Eqs. (20a)–(20c), the expression for the potential enstrophy reduces to

$$\sqrt{\varepsilon}_{adia} = \frac{\omega_{ci}^2 l_{mix}^2}{\hat{\alpha}} \left[\left(\frac{dn}{dx} - \frac{du}{dx} \right)^2 - \omega_{ci} \frac{dn}{dx} \left(\frac{dn}{dx} - \frac{du}{dx} \right) \right]. \tag{28}$$

The second term on the RHS of Eq. (28) arises from the contribution of the residual stress Π_{adia}^{res}. For a constant mixing length, $\sqrt{\varepsilon}_{adia}$ is proportional to $1/\hat{\alpha}$.

In the hydrodynamic limit: the expression for the turbulent potential enstrophy is obtained from Eqs. (24a)–(24c) as

$$\sqrt{\varepsilon}_{hydro} = \frac{\omega_{ci}^2 l_{mix}^2}{\sqrt{|\omega^\star|\hat{\alpha}}} \left(\frac{dn}{dx} - \frac{du}{dx} \right)^2 \propto \frac{1}{\sqrt{\hat{\alpha}}}. \tag{29}$$

Here, $\sqrt{\varepsilon}_{hydro}$ is proportional to $1/\sqrt{\hat{\alpha}}$. Note that in the hydrodynamic limit, the contribution of the residual stress to the expression for ε vanishes, as $\Pi_{hydro}^{res} \propto \sqrt{\hat{\alpha}} \to 0$. A comparison of Eqs. (28) and (29) shows that, in the adiabatic limit, the potential enstrophy is low, while ε is enhanced in the hydrodynamic limit. This is one reason why mesoscopic zonal flows are strong in the former case, while a state of enhanced turbulence dominates in the hydrodynamic limit. In summary, the equations of the simplified model in the adiabatic and hydrodynamic limits are

$$\partial_t n = -\partial_x \Gamma_n + D_0 \nabla^2 n, \tag{30a}$$

$$\partial_t u = -\partial_x \Pi + \mu_0 \nabla^2 u. \tag{30b}$$

The expressions for the particle and vorticity fluxes are

$$\Gamma_n^{adia} = -\frac{\varepsilon l_{mix}^2}{\hat{\alpha}} \frac{dn}{dx}, \tag{31a}$$

$$\Pi^{adia} = -\frac{\varepsilon l_{mix}^2}{\hat{\alpha}} \frac{du}{dx} - \frac{\omega_{ci} \varepsilon l_{mix}^2}{\hat{\alpha}} \frac{dn}{dx}, \tag{31b}$$

$$\sqrt{\varepsilon}_{adia} = \frac{l_{mix}^2}{\hat{\alpha}} \left[\left(\frac{dn}{dx} - \frac{du}{dx} \right)^2 - \omega_{ci} \frac{dn}{dx} \left(\frac{dn}{dx} - \frac{du}{dx} \right) \right], \tag{31c}$$

in the adiabatic limit, and

$$\Gamma_n^{hydro} = -\frac{\varepsilon l_{mix}^2}{\sqrt{\hat{\alpha}|\omega^\star|}} \frac{dn}{dx}, \tag{32a}$$

$$\Pi^{hydro} = -\frac{\varepsilon l_{mix}^2}{\sqrt{\hat{\alpha}|dn/dx|}} \frac{du}{dx} - \frac{\omega_{ci} \varepsilon \sqrt{\hat{\alpha}} l_{mix}^2}{|\omega^\star|^{3/2}} \frac{dn}{dx}, \tag{32b}$$

$$\sqrt{\varepsilon}_{hydro} = \frac{l_{mix}^2}{\sqrt{|\omega^\star|\hat{\alpha}}} \left(\frac{dn}{dx} - \frac{du}{dx} \right)^2, \tag{32c}$$

in the hydrodynamic limit.

An examination of the turbulence suppression criterion R_{DT} previously introduced in Ref. 24 as

$$R_{DT} = \frac{\int \partial_x \langle \tilde{v}_x \nabla^2 \tilde{\phi} \rangle \nabla \bar{v}_y dx}{-\int \langle \tilde{n} \tilde{v}_x \rangle dx}, \tag{33}$$

shows that R_{DT} decreases in the hydrodynamic limit. Here, R_{DT} is interpreted as the ratio of the turbulent enstrophy destruction rate $1/\tau_{transfer}$ due to coupling to the zonal flow through the vorticity flux or the Reynolds stress, as compared the turbulent enstrophy production rate $1/\tau_{relax}$ due to the relaxation of the density gradient. In the hydrodynamic limit, $1/\tau_{transfer}$ decreases because zonal flow production weakens.

VI. FATE OF ZONAL FLOWS IN THE HYDRODYNAMIC LIMIT $\alpha \ll 1$

Numerical studies of the evolution of resistive DW turbulence in the HW model show an enhancement of turbulence and a collapse of the zonal flows for hydrodynamic electrons.[18] As α decreases, the ratio of the kinetic energy of the zonal flow ($F \equiv 1/2 \int (\partial \langle \phi \rangle / \partial x)^2 dxdy$) to the total kinetic energy ($E^k \equiv 1/2 \int |\nabla \phi|^2 dxdy$) decreases, showing a transition of the plasma to a turbulence dominated state. In other words, when α drops below unity, zonal flows collapse and turbulent fluctuations are enhanced. To explain these observations, we present physical pictures that illustrate the sequence of events leading to the enhancement of turbulence and to the collapse of the shear layer in the hydrodynamic electron limit.

A. Physical picture: Energy-momentum flux physics

A useful insight into why zonal flow production is weaker in the hydrodynamic regime than in the adiabatic limit may be gleaned from the wave dispersion relation. In the adiabatic regime, the standard drift wave dispersion relation directly links radial propagation (related to group

velocity) to Reynolds stress $\langle \tilde{v}_x \tilde{v}_y \rangle$. In this limit, $|\omega^r| \gg |\gamma_m|$, suggesting the range of wave propagation is large. The expression for the Reynolds stress is

$$\langle \tilde{v}_x \tilde{v}_y \rangle = \sum_k i k_r i k_\theta \frac{c^2}{B^2} |\tilde{\phi}_k|^2 = -\sum_k k_r k_\theta \frac{c^2}{B^2} |\tilde{\phi}_k|^2, \quad (34)$$

where k_r and k_θ are the radial and azimuthal wavenumbers, respectively. The wave energy density flux $\langle v_{gr} \varepsilon \rangle$ is obtained by multiplying the group velocity $v_{gr} = -2\rho_s^2 k_r k_\theta v_d / (1 + k_\perp^2 \rho_s^2)^2$ by the energy

$$\langle v_{gr} \varepsilon \rangle = \sum_k -2\rho_s^2 \frac{k_r k_\theta v_d}{(1 + k_\perp^2 \rho_s^2)^2} \times (1 + k_\perp^2 \rho_s^2) \left(\frac{e\tilde{\phi}}{T_e} \right)^2 \frac{\rho_s^2 c_s^2}{2}, \quad (35a)$$

$$= \sum_k -\rho_s^4 c_s^2 \left(\frac{e\tilde{\phi}}{T_e} \right)^2 \frac{k_r k_\theta v_d}{1 + k_\perp^2 \rho_s^2}. \quad (35b)$$

With the electron diamagnetic velocity $v_d < 0$, and the group velocity $v_{gr} > 0$, the correlator $k_r k_\theta$ must be positive. This is to satisfy the causality condition that waves (for $r > r_0$) be outgoing from the region of excitation at $r \simeq r_0$. The Reynolds stress $\langle \tilde{v}_x \tilde{v}_y \rangle$ is thus < 0, while the energy flux $\langle v_{gr} \varepsilon \rangle$ is > 0. The causality relation implies a counter flow spin-up, suggesting that for outgoing wave energy flux, there exists an incoming wave momentum flux, as shown in Fig. 1. Note this depends on only the most basic aspects of the drift wave frequency.

In the hydrodynamic regime, however, the link of wave energy flux to Reynolds stress is broken. The momentum flux is still given by Eq. (34), but the group velocity v_{gr} is

$$v_{gr} = \frac{\partial \omega^r_{hydro}}{\partial k_r} = -\frac{k_r}{k_\perp^2} \omega^r_{hydro}.$$

Note here that causality has no implication for $\langle k_\theta k_r \rangle$, and neither for the Reynolds stress, since v_{gr} does not scale directly with k_θ (the wavenumber in the direction of symmetry). In the hydrodynamic limit, there is no causality constraint on the direction of eddy tilt, so the familiar tilt and stretch mechanism in not effective. Moreover, the waves have $|\omega^r| = |\gamma_m|$, suggesting the limited range of propagation.

B. Scalings of transport fluxes with α

When the adiabaticity parameter α decreases below unity, the system passes from the adiabatic to the hydrodynamic regime. According to the scalings of Eqs. (20) and (24), the particle flux scaling changes from $\Gamma_{adia} \propto 1/\alpha$ with $\alpha > 1$ to $\Gamma_{hydro} \propto \sqrt{1/\alpha}$ with $\alpha < 1$. The turbulent diffusivity χ_y that relates the vorticity flux to the vorticity gradient also exhibits the same scaling. The residual stress on the other hand drops from $\Pi^{res}_{adia} \propto 1/\alpha$ to $\Pi^{res}_{hydro} \propto \sqrt{\alpha}$. Scalings of the transport fluxes are summarized in Table I. An interpretation of the analytical results shows that the Reynolds power (which generates the zonal flow underlying suppression) drops with α. In the absence of external momentum sources and for turbulence, the diffusive vorticity flux balances the residual stress. The mean vorticity gradient shown in Fig. 2 then equals

TABLE I. Scalings of the turbulent enstrophy ε, transport fluxes, and vorticity gradient with α in both adiabatic and hydrodynamic regimes.

Plasma response	Adiabatic $\alpha \gg 1$	Hydrodynamic $\alpha \ll 1$
Turbulent enstrophy $\sqrt{\varepsilon}$	$\sqrt{\varepsilon} \propto 1/\alpha$	$\sqrt{\varepsilon} \propto 1/\sqrt{\alpha}$
Particle flux	Equation (20a)	Equation (24a)
Γ	$\Gamma \propto 1/\alpha$	$\Gamma \propto 1/\sqrt{\alpha}$
Turbulent viscosity	Equation (20b)	Equation (24b)
χ_y	$\chi_y \propto 1/\alpha$	$\chi_y \propto 1/\sqrt{\alpha}$
Residual stress	Equation (20c)	Equation (24c)
Π^{res}	$\Pi^{res} \propto -1/\alpha$	$\Pi^{res} \propto -\sqrt{\alpha}$
$\frac{\Pi^{res}}{\chi_y} = (\omega_{ci} \nabla \bar{n}) \times$	$\left(\frac{\alpha}{\lvert\omega^\star\rvert} \right)^0$	$\left(\frac{\alpha}{\lvert\omega^\star\rvert} \right)$

$$-\chi_y \frac{d^2 \bar{v}_y}{dx^2} + \Pi^{res} = 0 \Rightarrow \frac{d\nabla \bar{v}_y}{dx} = \frac{\Pi^{res}}{\chi_y}. \quad (36)$$

Figure 2 explains the significance of the vorticity gradient as a measure of the net strength of the shear layer. In the adiabatic limit, the ratio between the residual stress and the turbulent viscosity is independent of α. In the hydrodynamic limit, Π^{res}/χ_y is directly proportional to α. As the plasma transitions from the adiabatic to the hydrodynamic regime, the residual stress Π^{res} weakens, while the turbulent diffusivity χ_y increases. As a result, the ratio Π^{res}/χ_y—which indicates the plasma capacity to produce mesoscopic flows—drops. When the plasma production of zonal flows drops,

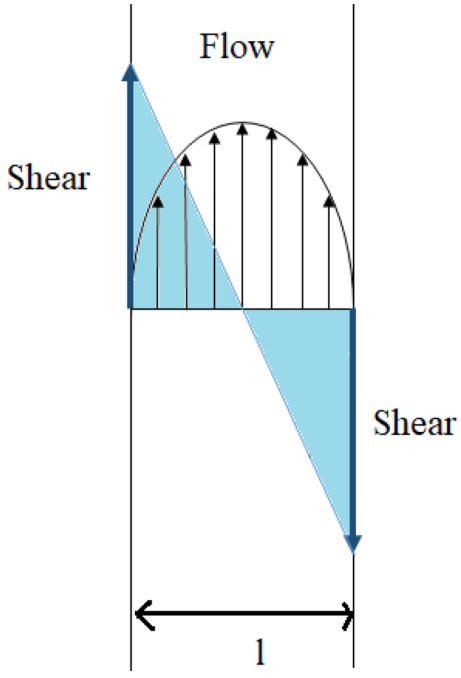

FIG. 2. A jump in the flow shear (in blue) over a scale length l is equivalent to a vorticity gradient on that scale.

turbulence is not effectively regulated and anomalous transport increases.

C. Potential vorticity mixing and zonal shear collapse

It is useful to examine the flow generation in the adiabatic and hydrodynamic regimes from the perspective of potential vorticity (PV) dynamics. The key concept here is that zonal flows are formed as a consequence of PV mixing,[3] which in a system with mean inhomogeneity necessitates trade-offs between mean and fluctuating PV. The classic example follows from the observation that for a rotating flow, the total vorticity: $\vec{\omega} + 2\vec{\Omega}$ is frozen into the fluid. If $\vec{\Omega} = \vec{\Omega}(\mathbf{x})$ changes, (due, say, to a variation in the axis of rotation relative to the plane of motion), a displacement of a mean vortex element in latitude forces a conversion of planetary vorticity ($\approx 2\vec{\Omega}$) to local flow vorticity ($\approx \vec{\omega}$), in order to conserve total PV. This produces a change in vorticity, while conserving total PV. This reasoning is the underpinning of the β plane model, for which the potential vorticity

$$q = \nabla_\perp^2 \phi + \beta y,$$

is conserved. That statement yields the familiar governing equation, which is

$$\partial_t \nabla_\perp^2 \phi + \nabla_\perp \phi \times \hat{z}.\nabla_\perp(\nabla_\perp^2 \phi) = -\beta V_y. \tag{37}$$

In the Hasegawa-Wakatani system, the conserved PV is: $\ln(n) - \nabla^2\phi$ which may be expanded to

$$q = \ln(n_0(x)) + \frac{\tilde{n}}{n_0} - \rho_s^2 \nabla^2 \left(\frac{|e|\phi}{T_e} \right).$$

Since $\tilde{n}/n_0 = |e|\tilde{\phi}/T_e + h$, it follows that

$$q = \ln(n_0(x)) + \frac{|e|\tilde{\phi}}{T_e} + h - \rho_s^2 \nabla^2 \left(\frac{|e|\phi}{T_e} \right),$$

so that Γ_q, the PV flux, is equal to

$$\Gamma_q = \langle \tilde{v}_x h \rangle - \rho_s^2 \left\langle \tilde{v}_x \nabla_\perp^2 \left(\frac{|e|\tilde{\phi}}{T_e} \right) \right\rangle. \tag{38}$$

Observe that the adiabatic part of the density perturbation makes no contribution to net PV flux or mixing. In the HW system, the displacement of a mean density element (analogous to the displacement of an element of planetary vorticity as shown in Fig. 3) induces a particle flux *and* a Reynolds force (from the vorticity flux), which drives a zonal flow. The latter follows from Taylor identity, assuming poloidal symmetry. Now in the adiabatic limit, density and vorticity fluctuations are tightly coupled. Indeed, both particle and vorticity evolution scale with α. Thus, it is not surprising that both particle flux and residual stress (i.e., the non-viscous component of the Reynolds force) scale identically ($\sim 1/\alpha$), and so zonal flows are robust. In the adiabatic regime, the particle flux and the vorticity flux support the PV flux. However, in the hydrodynamic regime, coupling of particle and PV fluctuations is weak [$\sim \mathcal{O}(\alpha)$ with $\alpha < 1$], so the respective fluxes can decouple. The PV flux is supported primarily by the particle flux $\Gamma_n \sim 1/\sqrt{\alpha}$, while the residual stress $\Pi^{res} \sim \sqrt{\alpha}$ is insignificant, with $\alpha \ll 1$. Thus, the non-diffusive Reynolds force drops with α, and so does flow production. Finally, the zonal vorticity gradient, an indication of the flow production, is proportional to α, suggesting that zonal flows and turbulence regulation are weak in the hydrodynamic regime. This is consistent with the findings of several numerical simulations, which conclude that zonal flows are robust for adiabatic electrons, but disappear in the hydrodynamic regime.[17–19] PV mixing (resulting from convective cell instability) persists in the hydrodynamic regime, but it is supported primarily by the particle flux, not vorticity transport.

VII. RELEVANCE TO DENSITY LIMIT n_G

The Greenwald density limit n_G is an operational bound on the plasma density and pressure. It represents the maximum attainable density before the plasma develops strong disruptions and MHD activity.[8,9] Experiments in various toroidal devices[6] including a recent experiment in the HL-2A tokamak[7] indicate a reduction of the edge shear flow layer and a strong enhancement of turbulent particle transport as $\bar{n} \to n_G$. The shearing rate of the mean $E \times B$ flow $\omega_{sh} = \nabla v_\theta$ drops, and the turbulent Reynolds power collapses in those ohmic L-mode discharges approaching n_G. In addition, both the core plasma density and the edge turbulent particle flux $\langle \tilde{v}_x \tilde{n} \rangle$ increase with $\bar{n}$. Meanwhile, the cross-correlation between the velocity and the density fluctuations grows substantially inside the separatrix. The core plasma temperature T_e on the other hand decreases with $\bar{n}$. Most importantly, the adiabaticity parameter α drops from 3 to 0.5 as $\bar{n}$ approaches n_G.[7] Note that in this particular HL-2A experiment, the plasma $\beta = 2\mu_0 p_e/B^2$ was very low, in the range: $0.01 < \beta < 0.02$.

The aforementioned experimental findings can be interpreted according to the scalings of Sec. VI. When the local edge plasma density increases, the adiabaticity parameter $\alpha(\propto T_e^2/\bar{n})$ decreases below unity, thereby triggering a plasma transition from the adiabatic to the hydrodynamic drift wave regime. According to the scalings of Sec. VI, this transition is associated with an increase in the turbulent particle flux and turbulence. Consistent with this, the mean vorticity gradient $d\nabla \bar{v}_y/dx = \Pi^{res}/\chi_y$ drops. The production of zonal flows thus declines, so turbulence is no longer

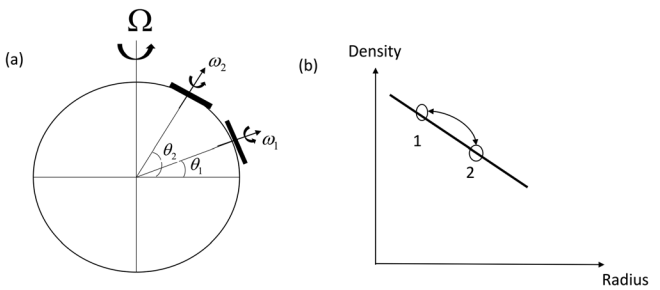

FIG. 3. Analogy of PV conservation in geostrophic waves and drift waves: (a) change in local vorticity $\vec{\omega}$ of a fluid element between θ_1 and θ_2 forces a flow generation, (b) density variation along the ∇n line from position 1 to position 2 triggers a change in the flow (i.e., vorticity) so to conserve q.

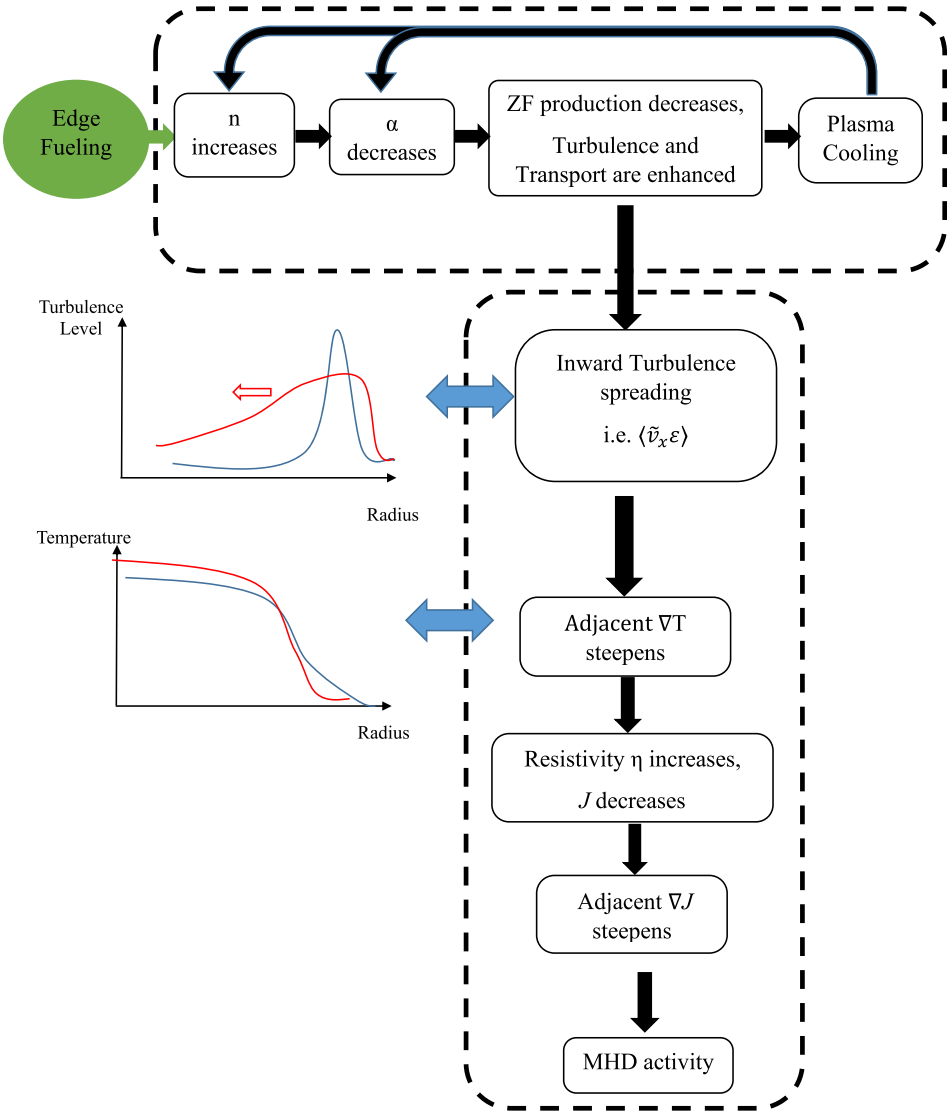

FIG. 4. Profile evolution in the hydrodynamic limit. The diagram shows a feedback loop between the density and temperature via variations of α. A potential path for the development of MHD modes involving turbulence spreading is also indicated. Inward turbulence spreading and steepening of adjacent ∇T from a state ① (in blue) to a state ② (in red) are shown on the left.

regulated effectively. Particle transport increases. For collisional drift waves, so does the electron thermal diffusivity, as particle and heat losses are comparable for that system. This need not be the case of Trapped Electron Modes (TEM), Ion Temperature Gradient (ITG), and other modes relevant to lower collisionality regimes. Cooling of the edge plasma is triggered. For constant pressure p_e (i.e., time scales long compared to a sound transit time), this leads to further increase in the density $\bar{n}$. A feedback loop between $\bar{n}$ and T_e is thus formed when α drops below unity. This scenario is summarized in the upper feedback loop in Fig. 4. We note that this scenario for the density limit does not necessarily require a MARFE or a disruption. It hinges only upon a change in the turbulence self regulation and particle transport for α decreases from $\alpha > 1$ to $\alpha < 1$. In addition, a path for the development of MHD activity is suggested. We suggest that such development can be promoted by turbulence spreading, which extends the region of degraded confinement inward from the edge, beyond the zone of initial zonal flow collapse. We propose that when the turbulence spreads inward, the temperature gradient will soften, causing the immediately adjacent ∇T to steepen. The resistivity then increases, and the adjacent ∇J also steepens, possibly triggering MHD activity. Note however, that this is simply a "scenario." Further work is needed in order to realize and validate it. And surely other scenarios, which link the increase in particle transport as $\bar{n}/n_G \to 1$ to MHD and disruptions, are possible.

This interpretation relies on the decrease in α below unity as the trigger for the drop in zonal flow production. Such an interpretation does not require appeal to zonal flow damping effects, associated with collisionality, charge exchange, etc. Most importantly, in contrast to Ref. 13, which postulates the surge in turbulence as due to yet another linear instability—such as the resistive ballooning mode—the current approach explains how variations of α affect the mean and turbulent plasma profiles within the context of generic drift wave theory. This mechanism is applicable to plasmas at low β, like that of the HL-2A experiment,[7] where resistive ballooning effects are not relevant.

VIII. CONCLUSION

This paper presents a theory of the collapse of a zonal shear layer in the hydrodynamic electron limit. It elucidates the evolution of the plasma flow and turbulence, as the electron response passes from the adiabatic to the hydrodynamic

limit. In particular, this paper describes the variation of the turbulent fluxes and mean profiles with the adiabaticity parameter $\alpha = k_z^2 v_{th}^2/(\nu_{ei}|\omega|)$. The key result of this paper is its explanation of why the zonal shear layer weakens and disappears when the adiabaticity parameter drops below unity, and so allows an enhanced level of turbulence. Moreover, this paper highlights the importance of the ZF collapse in the hydrodynamic limit ($\alpha < 1$) as a key mechanism and a general scenario for turbulence enhancement, even for plasmas with low β. We give a theoretical interpretation of the experimental and numerical results obtained in the hydrodynamic plasma limit. Findings of this paper are applicable to low β density limit experiments, where a weakening of the edge shear layer and a degradation of the thermal confinement result when the plasma density increases sufficiently so that $\alpha < 1$.

This paper presents a 1D reduced model that self-consistently describes the spatiotemporal evolution of the mean density $\bar{n}$ and the azimuthal flow $\bar{v}_y$, as well as the potential enstrophy $\varepsilon = \langle(\tilde{n} - \tilde{u})^2\rangle/2$. The model is derived from the Hasegawa-Wakatani system for turbulent drift waves and exploits conservation of PV to constrain the relation between drift waves and zonal flows. Key results of this paper are:

1. The particle flux Γ_n and the vorticity flux Π are calculated as: $\Gamma_n = -D\nabla\bar{n}$ and $\Pi = -\chi_y \nabla^2 \bar{v}_y + \Pi^{res}$. The vorticity flux is related to the Reynolds force via the Taylor identity. Quasi-linear analysis shows that the scalings of Γ_n and Π with α change as the plasma passes from the adiabatic to the hydrodynamic limit. These scalings are summarized in Table I and reveal the enhancement of the particle flux Γ_n and the turbulent viscosity χ_y as α decreases. The residual stress Π^{res} on the other hand drops with α for $\alpha \ll 1$ as $\Pi^{res}_{hydro} \propto \sqrt{\alpha}$.
2. Variations in the turbulent fluxes are responsible for the change in the mesoscopic flow dynamics. When α drops, the mean vorticity gradient $d(\nabla\bar{v}_y)/dx = \Pi_{res}/\chi_y$—which characterizes the zonal flow and the state of turbulence in the plasma—also drops. In the adiabatic limit, the mean vorticity gradient is independent of α. However, in the hydrodynamic limit, Π^{res}/χ_y is proportional to α, indicating weakened production of zonal flows for lower α. As the production of zonal flows decreases, the mechanism of self-regulation fails, and the turbulence intensity rises.
3. The findings of this paper illuminate several aspects of the physics of the density limit. When the plasma density increases, the adiabaticity parameter decreases ($\alpha \propto T_e^2/\bar{n}$). According to the scalings derived in Sec. VI, a decrease in the mean vorticity gradient results when $\bar{n}$ increases such that $\alpha \ll 1$. In this case, the *efficiency of the zonal flow production* drops. Thermal and particle losses due to collisional drift waves thus increase, and the cross phase between the velocity and the density fluctuations also increases.[7] Cooling of the plasma edge is then triggered, causing T_e to drop further. Feedback between $\bar{n}$ and T_e occurs.
4. Important results in this paper are the expressions for the fluxes Γ and Π. These expressions can be used to model the gradual plasma transition from the adiabatic to the hydrodynamic limit. While previous work simply presented numerical observations of the enhancement of turbulence,[17,18] no previous works presented a continuous transition from one limit to the other.
5. This paper gives a simple physical picture of why ZF production drops in the hydrodynamic electron regime. There the dispersion relation is $\omega_r^{hydro} = \sqrt{\omega^\star \hat{\alpha}/(2k_\perp^2\rho_s^2)}$, so $v_{gr} = -k_r \omega^r_{hydro}/k_\perp^2$. These are in contrast to the adiabatic case, for which $\omega_r^{adia} = \omega^\star(1 + k_\perp^2\rho_s^2)^{-1}$ and $v_{gr} = -2\rho_s^2 k_r k_\theta v_d/(1 + k_\perp^2\rho_s^2)^2$. Thus, in the hydrodynamic regime, the condition of outgoing waves ($v_{gr} > 0$) does not constrain the Reynolds stress $\langle\tilde{v}_x\tilde{v}_y\rangle \simeq \langle k_r k_\theta\rangle$, thus breaking the direct proportionality between wave propagation and Reynolds stress. This link is fundamental to ZF production by DWs.
6. This paper explains why turbulence is enhanced in the hydrodynamic limit and ascertains the physics of the Reynolds stress in regulating the drift wave—zonal flow relation. We show that PV mixing in the hydrodynamic electron limit is supported by the particle flux, i.e., $\langle\tilde{v}_x\tilde{q}\rangle = \langle\tilde{v}_x h\rangle - \langle\tilde{v}_x\nabla^2\tilde{\phi}\rangle \simeq \langle\tilde{v}_x h\rangle$. The vorticity flux drops and the particle flux rises with α in this regime. This explains why zonal flow formation is weak in the hydrodynamic regime.

At this point, it is necessary to add a brief answer to the inevitable questions: "What of the *H*-mode? Why doesn't the system transit to the *H*-mode when zonal flows are produced?." The answer to the latter is simple—the shear flows are not strong enough, for *L*-modes levels of edge heat flux. As the heat flux increases to the critical value for transition, the zonal shears become strong enough to induce a strong reduction in turbulence or turbulence collapse,[30,31] thus allowing ∇p_i to steepen and produce a mean $E \times B$ shear which "locks in" the *H*-mode trasnport barrier. The answer to the former is that the considerations of this paper (and numerous related works) suggest that the states of edge turbulence and particle transport and profiles may be classified as:

(i) a "normal," *L*-mode state where turbulence generated secondary modes (i.e., ZFs and GAMs) regulate turbulence and transport, but do not suppress them.
(ii) a *H*-mode state where the mean $E \times B$ shear, largely set by $\nabla\langle p_i\rangle$, is strong enough to suppress turbulence and turbulent transport. In *H*-mode, secondary modes are of little relevance, since primary mode levels are weak.
(iii) a state of degraded particle confinement, associated with the density limit. This state evolves from *L*-mode, and is accessed by reduction in secondary zonal flow production when $\alpha < 1$. In this state, turbulence and particle transport are large. Experiments suggest this state of degraded particle confinement can be accessed from *H*-mode only following an $H \rightarrow L$ back transition.[9] Table II summarizes this discussion. Finally, we note in passing that this classification of states does not include the improved mode

TABLE II. Secondary modes and states of particle confinement.

State	Electrons	Turbulence regulation
Base state—*L*-mode	Adiabatic or collisionless $\alpha > 1$	Secondary modes (ZFs and GAMs)
H-mode	Irrelevant	Mean $E \times B$ shear (∇p_i)
Degraded particle confinement (density Limit)	Hydrodynamic $\alpha < 1$	None—ZF collapse due weak production for $\alpha < 1$

(*I*-mode).[32] This is because the understanding of *I*-mode physics is still developing. We note that the "improvement" in *I*-mode is in thermal confinement, but not particle confinement. Thus, for the purpose of *this* discussion centered on *particle transport*, the *I*-mode can be lumped into the *L*-mode category.

Future work includes numerical investigation of the evolution of a plasma transition from one limit to the other. Moreover, it would be instructive to investigate experimentally the causality relation between the drop in α and the drop in ZF production. In particular, it is useful to determine which occurs first. This would probe the predictions of the theory. One suggestion would be to verify the decrease in the calculated total Reynolds work, as $\bar{n}/n_G$ is raised. When the total Reynolds work decreases, energy transfer to the mean flow structures drops, so the fluctuations should grow. Another possible experiment consists of increasing the plasma density $\bar{n}$ and temperature T_e, such that the adiabaticity parameter $\alpha \propto T_e^2/\bar{n}$ remains constant (assuming the variations of the Coulomb logarithm are negligible). According to the theory presented above, no collapse of the zonal shear layer should be observed, simply because α does not change. One can also investigate the contribution of collisional damping effects by comparing the response with and without the damping factor. This is particularly useful to confirm the pivotal role of the Reynolds stress in the collapse of the zonal shear layer at the density limit. Additional work also should include investigation of the role of high edge ∇p and high β values in *H*-modes in the enhancement of turbulence and profile evolution in density limit experiments.

ACKNOWLEDGMENTS

The authors would like to thank Ö. D. Gürcan, M. Greenwald, R. Hong, Z. B. Guo, P. Hennequinn, C. Hidalgo, Rameswar Singh, and G. R. Tynan for useful discussions. This work was supported by the U.S. Department of Energy, Office of Science, Office of Fusion Energy Sciences, under Award No. DE-FG02-04ER54738.

[1]P. H. Diamond, S. I. Itoh, K. Itoh, and T. S. Hahm, "Zonal flows in plasma: A review," Plasma Phys. Controlled Fusion **47**(5), R35–R161 (2005).
[2]P. W. Terry, "Suppression of turbulence and transport by sheared flow," Rev. Mod. Phys. **72**, 109–165 (2000).
[3]W. Horton, "Drift waves and transport," Rev. Mod. Phys. **71**, 735–778 (1999).
[4]B. D. Scott, "Energetics of the interaction between electromagnetic E × B turbulence and zonal flows," New J. Phys. **7**(1), 92 (2005).
[5]E. J. Kim and P. H. Diamond, "Zonal flows and transient dynamics of the L-H transition," Phys. Rev. Lett. **90**, 185006 (2003).
[6]Y. Xu, D. Carralero, C. Hidalgo, S. Jachmich, P. Manz, E. Martines, B. van Milligen, M. A. Pedrosa, M. Ramisch, I. Shesterikov, C. Silva, M. Spolaore, U. Stroth, and N. Vianello, "Long-range correlations and edge transport bifurcation in fusion plasmas," Nucl. Fusion **51**(6), 063020 (2011).
[7]R. Hong, G. R. Tynan, P. H. Diamond, L. Nie, D. Guo, T. Long, R. Ke, Y. Wu, B. Yuan, M. Xu, and The HL-2A Team, "Edge shear flows and particle transport near the density limit of the HL-2A tokamak," Nucl. Fusion **58**(1), 016041 (2018).
[8]M. Greenwald, J. L. Terry, S. M. Wolfe1, S. Ejima, M. G. Bell, S. M. Kaye, and G. H. Neilson, "A new look at density limits in tokamaks," Nucl. Fusion **28**, 2199 (1988).
[9]M. Greenwald, "Density limits in toroidal plasmas," Plasma Phys. Controlled Fusion **44**, R27 (2002).
[10]P. Manz, M. Ramisch, and U. Stroth, "Physical mechanism behind zonal-flow generation in drift-wave turbulence," Phys. Rev. Lett. **103**, 165004 (2009).
[11]M. Xu, G. R. Tynan, P. H. Diamond, P. Manz, C. Holland, N. Fedorczak, S. C. Thakur, J. H. Yu, K. J. Zhao, J. Q. Dong, J. Cheng, W. Y. Hong, L. W. Yan, Q. W. Yang, X. M. Song, Y. Huang, L. Z. Cai, W. L. Zhong, Z. B. Shi, X. T. Ding, X. R. Duan, and Y. Liu, "Frequency-resolved nonlinear turbulent energy transfer into zonal flows in strongly heated L-mode plasmas in the HL-2A tokamak," Phys. Rev. Lett. **108**, 245001 (2012).
[12]B. LaBombard, "An interpretation of fluctuation induced transport derived from electrostatic probe measurements," Phys. Plasmas **9**, 1300 (2002).
[13]B. N. Rogers, J. F. Drake, and A. Zeiler, "Phase space of tokamak edge turbulence, the $L-H$ transition, and the formation of the edge pedestal," Phys. Rev. Lett. **81**, 4396–4399 (1998).
[14]M. Z. Tokar, "Synergy of anomalous transport and radiation in the density limit," Phys. Rev. Lett. **91**, 095001 (2003).
[15]M. Z. Tokar, F. A. Kelly, and X. Loozen, "Role of thermal instabilities and anomalous transport in threshold of detachment and multifacetted asymmetric radiation from the edge (MARFE)," Phys. Plasmas **12**(5), 052510 (2005).
[16]B. Schmid, P. Manz, M. Ramisch, and U. Stroth, "Collisional scaling of the energy transfer in drift-wave zonal flow turbulence," Phys. Rev. Lett. **118**, 055001 (2017).
[17]J. Kim and P. W. Terry, "Numerical investigation of frequency spectrum in the Hasegawa-Wakatani model," Phys. Plasmas **20**(10), 102303 (2013).
[18]R. Numata, R. Ball, and R. L. Dewar, "Bifurcation in electrostatic resistive drift wave turbulence," Phys. Plasmas **14**(10), 102312 (2007).
[19]S. J. Camargo, D. Biskamp, and B. D. Scott, "Resistive drift-wave turbulence," Phys. Plasmas **2**(1), 48–62 (1995).
[20]A. V. Pushkarev, W. J. T. Bos, and S. V. Nazarenko, "Zonal flow generation and its feedback on turbulence production in drift wave turbulence," Phys. Plasmas **20**(4), 042304 (2013).
[21]K. Ghantous and Ö. D. Gürcan, "Wave-number spectrum of dissipative drift waves and a transition scale," Phys. Rev. E **92**, 033107 (2015).
[22]A. Hasegawa and M. Wakatani, "Plasma edge turbulence," Phys. Rev. Lett. **50**, 682 (1983).
[23]A. Hasegawa and K. Mima, "Stationary spectrum of strong turbulence in magnetized nonuniform plasma," Phys. Rev. Lett. **39**, 205–208 (1977).
[24]R. J. Hajjar, P. H. Diamond, A. Ashourvan, and G. R. Tynan, "Modelling enhanced confinement in drift-wave turbulence," Phys. Plasmas **24**(6), 062106 (2017).
[25]A. Ashourvan, P. H. Diamond, and Ö. D. Gürcan, "Transport matrix for particles and momentum in collisional drift waves turbulence in linear plasma devices," Phys. Plasmas **23**(2), 022309 (2016).
[26]A. Ashourvan and P. H. Diamond, "How mesoscopic staircases condense to macroscopic barriers in confined plasma turbulence," Phys. Rev. E **94**, 051202 (2016).
[27]H. Biglari, P. H. Diamond, and P. W. Terry, "Influence of sheared poloidal rotation on edge turbulence," Phys. Fluids B **2**(1), 1–4 (1990).
[28]J. C. Li, P. H. Diamond, X. Q. Xu, and G. R. Tynan, "Dynamics of intrinsic axial flows in unsheared, uniform magnetic fields," Phys. Plasmas **23**(5), 052311 (2016).
[29]P. H. Diamond, O. D. Gurcan, T. S. Hahm, K. Miki, Y. Kosuga, and X. Garbet, "Momentum theorems and the structure of atmospheric jets and

zonal flows in plasmas," Plasma Phys. Controlled Fusion **50**(12), 124018 (2008).
[30]P. Manz, G. S. Xu, B. N. Wan, H. Q. Wang, H. Y. Guo, I. Cziegler, N. Fedorczak, C. Holland, S. H. Muller, S. C. Thakur, M. Xu, K. Miki, P. H. Diamond, and G. R. Tynan, "Zonal flow triggers the L-H transition in the experimental advanced superconducting tokamak," Phys. Plasmas **19**(7), 072311 (2012).
[31]L. Schmitz, L. Zeng, T. L. Rhodes, J. C. Hillesheim, E. J. Doyle, R. J. Groebner, W. A. Peebles, K. H. Burrell, and G. Wang, "Role of zonal flow predator-prey oscillations in triggering the transition to H-mode confinement," Phys. Rev. Lett. **108**, 155002 (2012).
[32]D. G. Whyte, A. E. Hubbard, J. W. Hughes, B. Lipschultz, J. E. Rice, E. S. Marmar, M. Greenwald, I. Cziegler, A. Dominguez, T. Golfinopoulos, N. Howard, L. Lin, R. M. McDermott, M. Porkolab, M. L. Reinke, J. Terry, N. Tsujii, S. Wolfe, S. Wukitch, Y. Lin, and the Alcator C-Mod Team, "I-mode: An H-mode energy confinement regime with L-mode particle transport in alcator C-mod," Nucl. Fusion **50**(10), 105005 (2010).